Formation Reconfiguration by Impulse Control Along Elliptic Orbit

Akira Ichikawa, Emeritus Professor, Kyoto University

Abstract In this paper the size parameter change of the relative orbit by an impulse along an elliptic orbit is considered. The norm of the input vector is minimized with respect to the impulse time. An application of formation reconstruction by three-impulse control is given.

インパルス制御による楕円軌道上のフォーメーション再構成

市川　朗　京都大学名誉教授

概要　本稿では、インパルスによる楕円軌道上の相対軌道のサイズパラメータ制御を行い、入力ベクトルのノルムをインパルス時間で最小化する。応用例として３インパルスによるフォーメーション再構成を紹介する。

1 Tschauner-Hempel equations

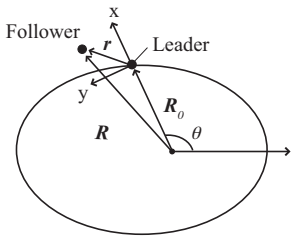

Fig. 1: Leader in elliptic orbit.

Tschauner-Hempel (TH) equations are linearized equations of relative motion along an elliptic orbit [1, 5, 7, 10–12] (see Fig.1) given by

$$\ddot{x} - 2\dot{\theta}\dot{y} - \ddot{\theta}y - (\dot{\theta}^2 + 2\frac{\mu}{R_0^3})x = u_x,$$
$$\ddot{y} + 2\dot{\theta}\dot{x} + \ddot{\theta}x - (\dot{\theta}^2 - \frac{\mu}{R_0^3})y = u_y,$$
$$\ddot{z} + \frac{\mu}{R_0^3}z = u_z,$$

where the elliptic orbit of the leader is $R_0 = \frac{p}{1+e\cos\theta}$, $R_0 = |\boldsymbol{R}_0|$, $\boldsymbol{R}_0$ is the position vector of the leader, $p = A_0(1-e^2)$ is the semilatus rectum, A_0 is the semi-major axis, e is the eccentricity of the orbit, θ is the true anomaly and μ is the gravitational constant of the earth. The orbital mean motion is $n = (\mu/A_0^3)^{1/2}$. For definiteness the perigee time is assumed to be $t_p = 0$ so that $\theta(0) = 0$. Introduce a non-dimensional time $\tau = t/(1/n)$ and set $\bar{\theta}(\tau) = \theta(\tau/n)$, $\bar{R}_0(\tau) = R_0(\tau/n)/A_0$, $\bar{x}(\tau = (1/A_0)x(\tau/n)$, $\bar{u}_x(\tau) = (1/A_0n^2)u_x(\tau/n)$ etc., the TH equations become non-dimensional

$$\bar{x}'' - 2\bar{\theta}'\bar{y}' - \bar{\theta}''\bar{y} - [(\bar{\theta}')^2\bar{x} + \frac{2}{\bar{R}_0^2}]\bar{x} = \bar{u}_x,$$
$$\bar{y}'' + 2\bar{\theta}'\bar{x}' + \bar{\theta}''\bar{x} - [(\bar{\theta}')^2 - \frac{1}{\bar{R}_0^2}]\bar{y} = \bar{u}_y,$$
$$\bar{z}'' + \frac{1}{\bar{R}_0^2}\bar{z} = \bar{u}_z,$$

where $'$ denotes the differentiation with respect to τ. For a given θ_0 the corresponding time τ_0 is given by

$$k_0(\tau - \tau_0) = \int_{\theta_0}^{\theta}\frac{d\theta}{\rho^2} = J(\theta,\theta_0), k_0 = (1-e^2)^{-3/2}.$$

The free motion of the TH equations was obtained by Yamanaka and Ankersen [13] using θ as the independent variable. The state transition matrix of the non-dimensional TH equations is given by

$$\Phi_{in}(\tau,\tau_0) = S_1(\theta)\Phi_{in}(\theta;\theta_0)\Phi_{in}^{-1}(\theta_0;\theta_0)S_1^{-1}(\theta_0),$$

$$\Phi_{out}(\tau,\tau_0)$$
$$= S_2(\theta)\begin{bmatrix}\cos(\theta-\theta_0) & \sin(\theta-\theta_0)\\ -\sin(\theta-\theta_0) & \cos(\theta-\theta_0)\end{bmatrix}S_2^{-1}(\theta_0),$$

where

$$S_1(\theta) = \begin{bmatrix}1/\rho & 0 & 0 & 0\\ 0 & 1/\rho & 0 & 0\\ k_0e\sin\theta & 0 & k_0\rho & 0\\ 0 & k_0e\sin\theta & 0 & k_0\rho\end{bmatrix},$$

$$S_2(\theta) = \begin{bmatrix}1/\rho & 0\\ k_0e\sin\theta & k_0\rho\end{bmatrix},$$

$$\Phi_{in}(\theta;\theta_0) =$$

$$\begin{bmatrix} s & c & 2-3esJ & 0 \\ (1+1/\rho)c & -(1+1/\rho)s & -3\rho^2 J & 1 \\ s' & c' & -3e(s'J+s/\rho^2) & 0 \\ -2s & -2c+e & -3(1-2esJ) & 0 \end{bmatrix},$$

$s = \rho\sin\theta,\ c = \rho\cos\theta,\ s' = -e\sin^2\theta + \rho\cos\theta,$

$c' = -e\sin\theta\cos\theta - \rho\sin\theta = (1-2\rho)\sin\theta.$

Define six parameters

$$\bar{\boldsymbol{K}}(\tau_0) = \begin{bmatrix} \Phi_{in}^{-1}(\theta_0;\theta_0)S_1^{-1}(\theta_0)\bar{\boldsymbol{x}}_{in}(\tau_0) \\ \Phi_{out}^{-1}(\theta_0;\theta_0)S_2^{-1}(\theta_0)\bar{\boldsymbol{x}}_{out}(\tau_0) \end{bmatrix}.$$

Then

$$\bar{x}(\tau) = \bar{K}_1(\tau_0)\sin\theta + \bar{K}_2(\tau_0)\cos\theta + \bar{K}_3(\tau_0)(2-3esJ)/\rho$$
$$= a_0\sin(\theta+\alpha_0) + \bar{K}_3(\tau_0)(2-3esJ)/\rho,$$
$$\bar{y}(\tau) = \bar{K}_1(\tau_0)(1+1/\rho)\cos\theta - \bar{K}_2(\tau_0)(1+1/\rho)\sin\theta$$
$$- 3\bar{K}_3(\tau_0)\rho J + \bar{K}_4(\tau_0)/\rho$$
$$= -(1+1/\rho)a_0\cos(\theta+\alpha_0) - 3\bar{K}_3(\tau_0)\rho J + \bar{K}_4(\tau_0)/\rho,$$
$$\bar{z}(\tau) = \frac{1}{\rho}[\bar{K}_5(\tau_0)\cos\theta + \bar{K}_6(\tau_0)\sin\theta$$
$$= \frac{1}{\rho}b_0\cos(\theta+\beta_0),$$

where $a_0 = (\bar{K}_1(\tau_0)^2 + \bar{K}_2(\tau_0)^2)^{1/2}$, $\bar{K}_1(\tau_0) = -a_0\sin\alpha_0$ and $\bar{K}_2(\tau_0) = a_0\cos\alpha_0$. $\bar{K}_3(\tau_0)$ is a parameter of the drifting motion. If it is zero, the in-plane motion is periodic and a_0 indicates its size. $\bar{K}_4(\tau_0)$ is a parameter of deviation from the origin. Graphical generation of periodic orbits is discussed in [2].

2 Impulse control of size parameter

The size parameters a_0 and b_0 are important factors in formation flying. In this section the follower satellite is assumed to be in a periodic orbit and the change of size parameter a_0 to a by a single impulse is considered. For simplicity $\tau_0 = 0$ and suppose that an impulse $\boldsymbol{u}_{in} = [u_x\ \ u_y]^T$ is applied at τ. Then parameters before and after the impulse are related by

$$\bar{\boldsymbol{K}}_{in}(\tau^+) = \Phi_{in}^{-1}(\theta;\theta)S^{-1}(\theta)(\bar{\boldsymbol{x}}_{in}(\tau) + [0\ \ 0\ \ u_x\ \ u_y]^T$$
$$= \bar{\boldsymbol{K}}_{in}(\tau) + \Phi_{in}^{-1}(\theta;\theta)S^{-1}(\theta)[0\ \ 0\ \ u_x\ \ u_y]^T,$$

where $\theta = \theta(\tau)$ and $\bar{\boldsymbol{K}}_{in}(\tau^+)$ is the parameter after the impulse. Assume

$$\begin{bmatrix} \bar{K}_{1+} \\ \bar{K}_{2+} \end{bmatrix} = \begin{bmatrix} -a\sin\alpha \\ a\cos\alpha \end{bmatrix}.$$

Then

$$\begin{bmatrix} \bar{K}_{1+} \\ \bar{K}_{2+} \end{bmatrix} = \begin{bmatrix} \bar{K}_1(0) \\ \bar{K}_2(0) \end{bmatrix}$$
$$+ \frac{1}{k_0\rho(1-e^2)}\begin{bmatrix} c-2e & -s(1+1/\rho) \\ -s & -c(1+1/\rho)-e \end{bmatrix}\begin{bmatrix} u_x \\ u_y \end{bmatrix},$$

where $\bar{K}_i(\tau) = \bar{K}_i(0)$ is used. This is always solved to yield

$$\begin{bmatrix} u_x \\ u_y \end{bmatrix} = -\frac{k_0\rho}{2}\begin{bmatrix} -(1+\rho)\cos\theta - e & (1+\rho)\sin\theta \\ s & c-2e \end{bmatrix}$$
$$\times \begin{bmatrix} \bar{K}_{1+} - \bar{K}_1(0) \\ \bar{K}_{2+} - \bar{K}_2(0) \end{bmatrix}.$$

Using size and phase parameters, this is rewritten as

$$[u_x\ \ u_y]^T =$$
$$\frac{k_0\rho}{2}\begin{bmatrix} (1+\rho)(a_0\sin(\theta+\alpha_0) - a\sin(\theta+\alpha)) \\ +e(a_0\sin\alpha_0 - a\sin\alpha) \\ \rho(a_0\cos(\theta+\alpha_0) - a\cos(\theta+\alpha)) \\ -2e(a_0\cos\alpha_0 - a\cos\alpha) \end{bmatrix}.$$

Now the minimum norm of this impulse vector is examined, where the 1-norm $||\boldsymbol{u}_{in}||_1 = |u_{x1}| + |u_{y1}|$ is used. $||\boldsymbol{u}_{in}||_1$ is minimized with respect to $\theta = \theta(\tau)$ and α. The main results of this paper is that the minimizing pair is $\alpha = \alpha_0$ and θ such that $u_x = 0$ for $e \le e_0(\alpha_0)$, the switching point. To show this, recall that $\boldsymbol{u}_{in}$ with $\alpha = \alpha_0$ is given by

$$\boldsymbol{u}_{in}(\tau) = \frac{k_0(a_0-a)}{2}\rho\begin{bmatrix} (1+\rho)\sin(\theta+\alpha_0) + e\sin\alpha_0 \\ \rho\cos(\theta+\alpha_0) - 2e\cos\alpha_0 \end{bmatrix}.$$

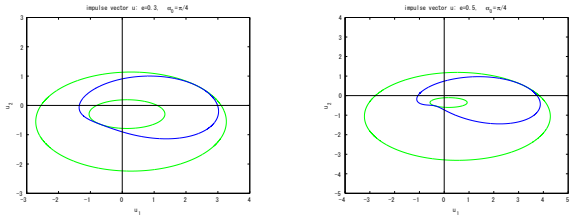

(a) $(e, \alpha_0) = (0.3, \pi/4)$ (b) $(e, \alpha_0) = (0.5, \pi/4)$

Fig. 2: Loci of vector $\boldsymbol{u}$.

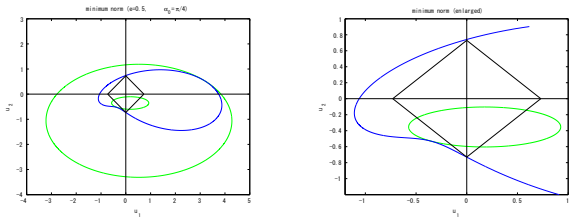

(a) $\boldsymbol{u}$ and square (b) enlarged

Fig. 3: Minimum norm $(u_1 = 0)$

Hence the minimum norm of

$$\boldsymbol{u} = \rho \begin{bmatrix} (1+\rho)\sin(\theta+\alpha_0) + e\sin\alpha_0 \\ \rho\cos(\theta+\alpha_0) - 2e\cos\alpha_0 \end{bmatrix}$$

is examined. Its locus E_u is given by

$$\left(\frac{u_1 - \rho e\sin\alpha_0}{a}\right)^2 + \left(\frac{u_2 + 2e\rho\cos\alpha_0}{b}\right)^2 = 1,$$

$$a = \rho(1+\rho), b = \rho^2$$

and lies between two ellipses E_s and E_S (see Fig.2)

$$\left(\frac{u_1 + e(1-e)\sin\alpha_0}{(1-e)(2-e)}\right)^2 + \left(\frac{u_2 - 2e(1-e)\cos\alpha_0}{(1-e)^2}\right)^2 = 1,$$

$$\left(\frac{u_1 + e(1+e)\sin\alpha_0}{(1+e)(2+e)}\right)^2 + \left(\frac{u_2 - 2(1+e)e\cos\alpha_0}{(1+e)^2}\right)^2 = 1.$$

Note that vector $\boldsymbol{u}$ is in contact with the larger and smaller ellipses respectively at $\theta = 0, \pi$. The unit "circle" with respect to the norm $||\boldsymbol{v}||_1 = |v_1| + |v_2|$ is the unit square rotated by $\pi/4$. The minimum norm of $\boldsymbol{u}$ is attained at the tangent point of E_u and some square $||\boldsymbol{v}||_1 = r$ see Fig.3. Obviously, when e is not large, the minimum is attained on the vertical axis where $u_1 = 0$. As e increases, the small ellipse E_s shrinks as can be seen from Fig.2. For $e > 0.6$ the minimum is not necessarily attained on the vertical axis. This is because the smaller ellipse becomes smaller and the contact point $\boldsymbol{u}(\pi)$ approaches the origin. Hence it is necessary to examine the properties of the locus E_u. The lemma below summarizes useful properties of the locus E_u.

Lemma 2.1. (i) $E_u(\pi - \alpha_0)$ is the π rotation of $E_u(\alpha_0)$ around the u_1 axis.
(ii) $E_u(\pi + \alpha_0)$ is the π rotation of $E_u(\alpha_0)$ around the origin and hence two loci are symmetric with respect to the origin.
(iii) $E_u(\pi/2)$ is symmetric with respect to the u_1 axis .
(iv) $E_u(0)$ $(E_u(\pi))$ is symmetric with respect to the u_2 axis.
(v) For $e = 0$, E_u is independent of α_0 and is given by the ellipse $(\frac{u_1}{2})^2 + u_2^2 = 1$.
(vi) For $e = 1$, $\boldsymbol{u}(\pi, \alpha_0) = 0$ for all α_0 and the smaller ellipse shrinks to the origin.

As a consequence of this lemma, the following is true.

Lemma 2.2. The family of loci $E_u(\alpha_0),\ 0 \le \alpha_0 < 2\pi$ can be generated by $E_u(\alpha_0),\ 0 \le \alpha_0 \le \pi/2$.

Due to this lemma, it suffices to examine the subfamily of loci $E_u(\alpha_0), 0 \le \alpha_0 \le \pi/2$. The minimizing θ and the minimum norm of $\boldsymbol{u}$ will be determined.

Lemma 2.3. For $0 \le e < 1$ and $0 \le \alpha_0 < 2\pi$, $u_1(\theta) = (1+\rho)\sin(\theta+\alpha_0) + e\sin\alpha_0$ has two zeros $\theta_1 < \theta_2$ on $[0\ \ 2\pi]$ and the modulus of $u_2(\theta) = \rho[\rho\cos(\theta+\alpha_0) - 2e\cos\alpha_0]$ is equal at these points.

Consider the subfamily $E_u(\alpha_0), 0 \le \alpha_0 \le \pi/2$. As a representative of this subfamily, $\alpha_0 = \pi/4$ will be discussed. Fig.4 is a collection of loci of $\boldsymbol{u}(\theta; \pi/4)$ with parameter e. When $e = 0$, the leader's orbit is circular. Moreover, the smaller ellipse shrinks to the origin. E_u is independent of α_0 and coincide with the larger ellipse as shown in Fig.4-(a). E_u for $e = 0.3$ is given by Fig.4-(b) and has egg-like shape, but as e increases, the smaller ellipse shrinks and E_u tangent to it at $\theta_3 = \pi$ is pulled towards the origin see Fig.4-(c). First confirm that the norm of $\boldsymbol{u}$ at two zeros of u_1 agree. Fig.5-(a) gives two zeros denoted by θ_1 and θ_2 of u_1 as functions of e. The norms of $\boldsymbol{u}$ at these two points denoted by v_1 and v_2 agree as seen from Fig.5-(b). The minimizing θ of the norm of $\boldsymbol{u}(\theta; \pi/4)$ is determined by direct search and is denoted by θ_0. For $e \ge 0.6$ there exists a θ in the neighborhood of π such that $du_2/du_1 = -1$ which is denoted by θ_4. Fig.6-(a) is the enlarged locus of $\boldsymbol{u}$ near the origin and Fig.6-(b) is the graph of $du_2/du_1 + 1$. $\boldsymbol{u}(\theta_4)$ is a contact point of E_u and $||\boldsymbol{v}||_1 = r$ for some

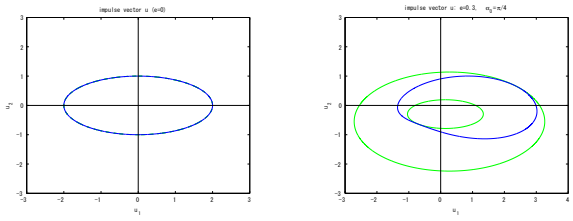

(a) $e = 0$ (b) $e = 0.3$

(c) $e = 0.5$ (d) $e = 0.7$

Fig. 4: Loci of $\boldsymbol{u}$ with parameter e.

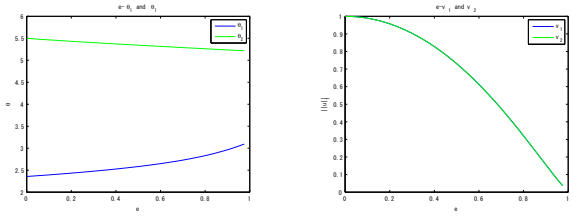

(a) Zeros of $u_1(\theta)$ (b) v_1 and v_2

Fig. 5: Zeros of u_1 and norm of $\boldsymbol{u}$ $(\alpha_0 = \pi/4)$

r. Fig.7-(a) depicts the graphs of θ_0, θ_1 and θ_4. For $e \leq 0.65$ θ_0 agrees with θ_1 and then switches to θ_4. Hence $e(\pi/4) = 0.65$. For $e \leq e(\pi/4)$, θ_2 is also minimizing, but in the graph, θ_1 is used. Fig.7-(b) gives norms $v_0 = ||\boldsymbol{u}(\theta_0)||_1$, $v_1 = ||\boldsymbol{u}(\theta_1)||_1$ and $v_4 = ||\boldsymbol{u}(\theta_4)||_1$. For $e \geq 0.65$, v_1 is no longer minimum but remains very close to v_0.

Now consider the general case with variable α. The impulse vector is

$$\boldsymbol{u}_{in} = \frac{k_0\rho}{2}\left(\begin{bmatrix} (1+\rho)(a_0\sin(\theta+\alpha_0) \\ \rho(a_0\cos(\theta+\alpha_0) - a\cos(\theta+\alpha)) \end{bmatrix} - \begin{bmatrix} a\sin(\theta+\alpha)) \\ 2e(a_0\cos\alpha_0 - a\cos\alpha) \end{bmatrix}\right)$$

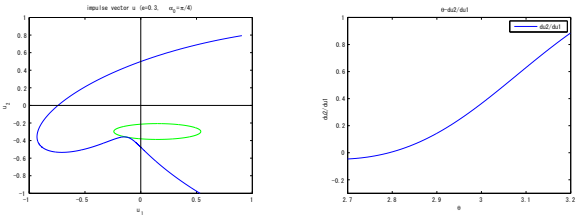

(a) $\boldsymbol{u}$ $(e = 0.7)$ (b) $du2/du1 + 1$: $(e = 0.65)$

Fig. 6: Enlarged locus and $du2/du1 + 1$ $(\alpha_0 = \pi/4)$

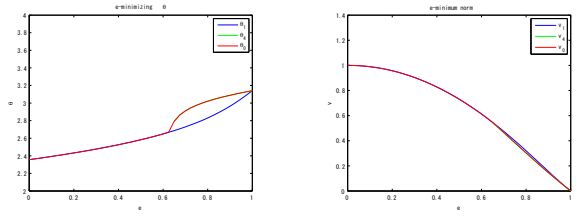

(a) Minimizing θ (b) Minimum norm

Fig. 7: Minimizing θ and minimum norm v $(\alpha_0 = \pi/4)$

Let $a = ra_0, r > 0$ and define

$$\boldsymbol{u}_\alpha = \rho\begin{bmatrix} (1+\rho)\sin(\theta+\alpha) + e\sin\alpha \\ \rho\cos(\theta+\alpha) - 2e\cos\alpha \end{bmatrix}$$

Then

$$\boldsymbol{u}_{in}(\tau) = \frac{a_0k_0}{2}(\boldsymbol{u}_{\alpha_0} - r\boldsymbol{u}_\alpha)(\theta)$$

Let $r = 1/2$ and consider

$$\boldsymbol{u} = \boldsymbol{u}_{\alpha_0} - r\boldsymbol{u}_\alpha$$

For a given α_0, the minimizing pair (α, θ) is sought by direct search. Fig.8 compares the pair in blue with (α_0, θ_1) in green previously obtained. There exists a switching point $e(\pi/4)$ such that for $e \leq e(\pi/4)$, θ_0 coincides with θ_1. Moreover, there exists $e_0(\pi/4) < e(\pi/4)$ such that for $e \leq e_0(\pi/4)$, the minimizing pair coincides with (α_0, θ_1). $e_0(\pi/4) \approx 0.6$ and for $e > e_0(\pi/4)$ $\alpha < \alpha_0$. When $\alpha_0 = 0$, $E_u(0)$ is symmetric with respect to the u_2 axis and $\theta_0 = \theta_1 = 0$ for all e. The minimizing pair $(\theta, \alpha) = (\theta_0, \alpha_0) = (0, 0)$. For $\alpha_0 = \pi/3, 5\pi/12, \pi/2$, Fig.9 depicts the minimizing pair and the minimum norm in blue and (θ_0, α_0) in green. For $\alpha_0 < 0.9$, θ_0 switches once from θ_1 to θ_4. For the larger value of α_0, θ_0 switches

twice from θ_2 to θ_4 and then to θ_3. See Fig.8-(c) with $\alpha_0 = 5\pi/12$. For every α_0, there exists $e(\alpha_0)$ such that for $e \le e(\alpha_0)$ θ_0 coincides with θ_1.There also exists $e_0(\alpha_0) < e(\alpha_0)$ such that for $e \le e_0(\alpha_0)$, the minimizing pair coincides with (α_0, θ_1). Both $e_0(\alpha_0)$ and $e(\alpha_0)$ are monotone decreasing in $0 < e < \pi/2$. When $\alpha_0 = \pi/2$, the minimizing pair coincides with (θ_0, α_0) for all e.
The transfer to a periodic orbit by a single impulse is considered in [7].

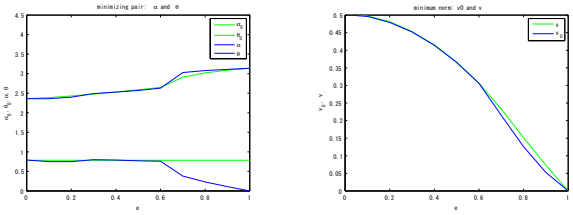

(a) $(\alpha, \theta) : (\alpha_0 = \pi/4)$ (b) $v : (\alpha_0 = \pi/4)$

Fig. 8: Minimizing pair and minimum norm v

As an application, consider the reconfiguration of the follower orbit from a periodic orbit with size a_0 to one with size a_f. Apply impulses $\boldsymbol{u}_i, i = 1, 2, 3$ at $\theta = \theta_1, \theta_2, \theta_3 = \theta_1 + 2\pi$, where

$$\boldsymbol{u}_i = \frac{k_0(a_i - a_{i-1})}{2} \begin{bmatrix} 0 \\ u_2(\theta_i) \end{bmatrix},$$

$$u_2(\theta) = \rho(\rho\cos(\theta + \alpha_0) - 2e\cos\alpha_0).$$

and $a_3 = a_f$. Let $\bar{K}_{ij}$ be the parameter $\bar{K}_i$ after the impulse $\boldsymbol{u}_j$. Then

$$\bar{K}_{13} = -a_f \sin\alpha_0 - 3e(J_{21}\bar{K}_{31} + J_{32}\bar{K}_{32}),$$

$$\bar{K}_{23} = a_f \cos\alpha_0,$$

$$\begin{aligned}\bar{K}_{33} = &\frac{a_0 - a_1}{2(1-e^2)} u_2(\theta_1)\rho^2 \\ &+ \frac{a_1 - a_2}{2(1-e^2)} u_2(\theta_2)\rho^2 \\ &+ \frac{a_2 - a_f}{2(1-e^2)} u_2(\theta_1)\rho^2,\end{aligned}$$

$$\begin{aligned}\bar{K}_{43} = &-3(J_{21}\bar{K}_{31} + J_{32}\bar{K}_{32}) - \frac{a_0 - a_1}{2(1-e^2)} u_2(\theta_1)e\rho\sin\theta_1 \\ &- \frac{a_1 - a_2}{2(1-e^2)} u_2(\theta_2)e\rho\sin\theta_2 \\ &- \frac{a_2 - a_f}{2(1-e^2)} u_2(\theta_1)e\rho\sin\theta_1,\end{aligned}$$

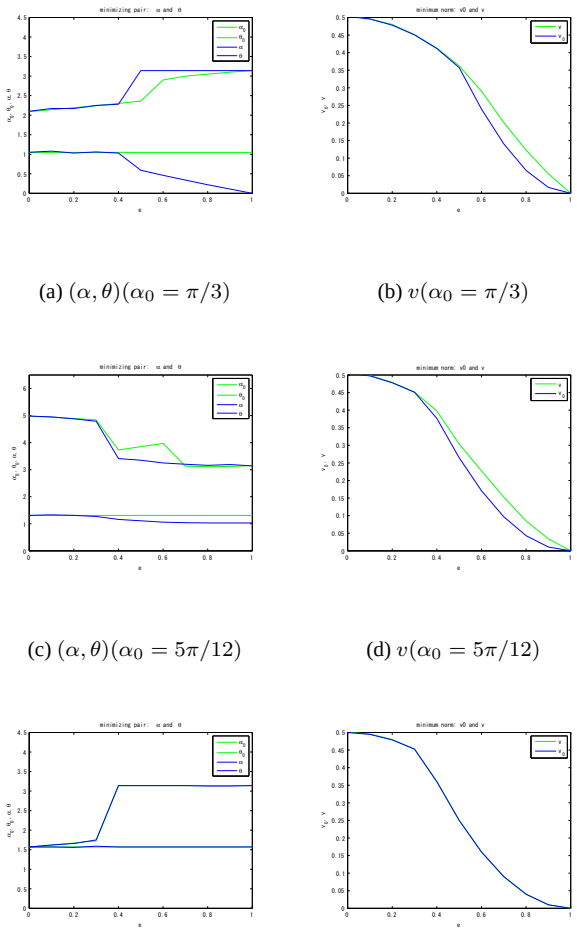

(a) $(\alpha, \theta)(\alpha_0 = \pi/3)$ (b) $v(\alpha_0 = \pi/3)$

(c) $(\alpha, \theta)(\alpha_0 = 5\pi/12)$ (d) $v(\alpha_0 = 5\pi/12)$

(e) $(\alpha, \theta)(\alpha_0 = \pi/2)$ (f) $v(\alpha_0 = \pi/2)$

Fig. 9: Minimizing pair and minimum norm

where $J_{ij} = J(\theta_i, \theta_j)$. To satisfy the requirement that the final orbit is periodic and the size parameter is a_f, free parameters a_1 and a_2 are chosen to satisfy

$$\bar{K}_{33} = 0$$

$$J_{21}\bar{K}_{31} + J_{32}\bar{K}_{32} = 0.$$

Two equations yield a linear equation for a_1 and a_2 which has a solution. Fig.10 shows three impulse trajectories changing the size from $a_0 = 0.001$ to $a_f = 0.005$. The parameters satisfy the inequality $a_0 > a_1 > a_2 > a_f$ and $\Delta V = |a_0 - a_f|k_0|u_2(\theta_1)|/2$. Simulation results are given in Fig.10. Impulse positions are indicated by red dots. Figs.10 (a) and (b) are the cases with $\alpha_0 = \pi/4$ and $e = 0.3$ and $e = 0.5$ respectively. The parameter α_0 is equal to $\pi/4$ for Figs.10 (c) and (d) and $\pi/2$ for Figs.10 (e) and (f). When the leader orbit is circular ($e = 0$), $\theta = nt = \tau$ and the minimum norm of $\boldsymbol{u}$ is at-

tained on the vertical axis. The impulse time is given by $\tau + \alpha_0 = \pi$ or $\tau + \alpha_0 = 2\pi$ which recovers the results in [6]. The three-impulse strategy given above is an optimal one for the open time minimum norm problem in [6] and $\Delta V = |a_0 - a_f|/2$. See also [8]. Note that for standard trajectory control the terminal time is fixed [3, 4, 9].

For $e > 0$, parameters $\bar{K}_1$ and $\bar{K}_4$ are time-varying when $\bar{K}_3$ is not equal to zero. Then the minimum norm problem involves J terms and further study is necessary for the open-time problem of TH equations.

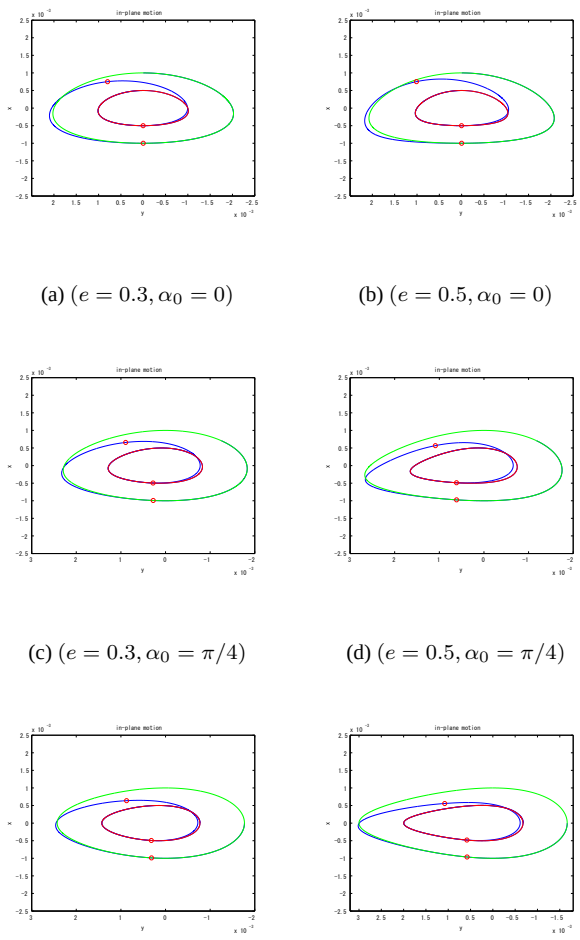

(a) $(e = 0.3, \alpha_0 = 0)$ (b) $(e = 0.5, \alpha_0 = 0)$

(c) $(e = 0.3, \alpha_0 = \pi/4)$ (d) $(e = 0.5, \alpha_0 = \pi/4)$

(e) $(e = 0.3, \alpha_0 = \pi/2)$ (f) $(e = 0.5, \alpha_0 = \pi/2)$

Fig. 10: Three impulse trajectories: $\bar{K}_{33} = 0$

References

[1] Alfriend, K. T., Vadali, S. R., Gurfil, P., How, J. P., and Breger, L. S., "*Spacecraft Formation Flying: Dynamics, Control and Navigation*," Elsevier, Amsterdam, 2010.

[2] Bando. M., and Ichikawa. A., "Graphical Generation of Periodic Orbits of Tschauner-Hempel Equations," *Journal of Guidance, Control, and Dynamics*, Vol. 35, No. 3, 2012, pp. 1002-1007.

[3] Carter, T. E., and Brient, J., "Fuel-Optimal Rendezvous Problem for Linearized Equations of Motion," *Journal of Guidance, Control, and Dynamics*, Vol. 15, No. 6, 1992, pp. 1411-1416.

[4] Carter, T. E., and Brient, J., "Linearized Impulsive Rendezvous Problem," *Journal of Optimization Theory and Applications*, Vol. 86, No. 3, 1995, pp. 553-584.

[5] Gurfil, P., "Relative Motion Between Elliptic Orbits: Generalized Boundedness Conditions and Optimal Formationkeeping," *Journal of Guidance, Control, and Dynamics*, Vol. 28, No. 4, 2005, pp. 761-767.

[6] Ichimura. Y., and Ichikawa. A., "Optimal Impulsive Relative Orbit Transfer Along a Circular Orbit," *Journal of Guidance, Control, and Dynamics*, Vol. 31, No. 4, 2008, pp. 1014-1027.

[7] Inalhan, G., Tillerson, M., and How, J. P., "Relative Dynamics and Control of Spacecraft Formations in Eccentric Orbits," *Journal of Guidance, Control, and Dynamics*, Vol. 25, No. 1, 2002, pp. 48-59.

[8] Jifuku, R., Ichikawa. A, and Bando, M., "Satellite Formation by Pulse Control Along a Circular Orbit", *Journal of Guidance, Control, and Dynamics*, Vol. 34, No. 5, 2012, pp. 1329-1341..

[9] Neustadt, L. W., "A General Theory of Minimum-Fuel Space Trajectories, SIAM Journal on control, Vol. 3, No. 2, 1965, pp. 317-356.

[10] Shibata, M., and Ichikawa. A., "Orbital Rendezvous and Flyaround Based on Null Controllability with Vanishing Energy," *Journal of Guidance, Control, and Dynamics*, Vol. 30, No. 4, 2007, pp. 934-945.

[11] Tschauner, J., and Hempel, P., "Rendezvous with a Target in an Elliptical Orbit," *Astronautica Acta*, Vol. 11, No. 2, 1965, pp. 104-109.

[12] Wie, B., "Space Vehicle Dynamics and Control," AIAA, Reston, Virginia, 1998, pp. 282-285.

[13] Yamanaka, K., and Ankersen, F., "New State Transition Matrix for Relative Motion on an Arbitrary Elliptical Orbit," *Journal of Guidance, Control, and Dynamics*, Vol. 25, No. 1, 2002, pp. 60-66.